

# Estimation of the Particle Deposition on a Subsonic Axial Compressor Blade

Alessio Suman<sup>1</sup>, Mirko Morini<sup>2</sup>, Rainer Kurz<sup>3</sup>, Nicola Aldi<sup>1</sup>, Klaus Brun<sup>4</sup>, Michele Pinelli<sup>1</sup>, Pier Ruggero Spina<sup>1</sup>

<sup>1</sup> Dipartimento di Ingegneria, Università degli Studi di Ferrara, Ferrara, Italy

<sup>2</sup> Dipartimento di Ingegneria Industriale, Università degli Studi di Parma, Parma, Italy

<sup>3</sup> Solar Turbines Incorporated, San Diego, CA, USA

<sup>4</sup> Southwest Research Institute, San Antonio, TX, USA

## ABSTRACT

The quality and purity of the air entering a gas turbine is a significant factor influencing its performance and life. Foulants in the ppm range which are not captured by the air filtration system usually cause deposits on blading, which results in a severe drop in the performance of the compressor.

Through the interdisciplinary approach proposed in this paper, it is possible to determine the evolution of the fouling phenomenon through the integration of studies in different research fields: (i) numerical simulation, (ii) power plant characteristics and (iii) particle-adhesion characteristics. In fact, the size of the particles, their concentrations and adhesion ability, and filtration efficiency represent the major contributors to performing a realistic quantitative analysis of fouling phenomena in an axial compressor. The aim of this work is the estimation of the actual deposits on the blade surface in terms of location and quantity. This study combines the impact/adhesion characteristic of the particles obtained through a CFD and the real size distribution of the contaminants in the air swallowed by the compressor.

The blade zones affected by deposits are clearly reported by using easy-to-use contaminant maps realized on the blade surface, in terms of contaminant mass.

The analysis has shown that particular fluid-dynamic phenomena and airfoil shape influence the pattern deposition. The use of a filtration system decreases the contamination of the blade and the charge level of the electrostatic seems to be less important than the air contaminant concentration. From these analyses, some guidelines for proper installation and management of the power plant (in terms of filtration systems and washing strategies) can be drawn up. Characterization of the air contaminants in the power plant location represents the most important step in improving the management of the gas turbine power plant.

## INTRODUCTION

Each manufacturer's gas turbine has its own tolerances and design constraints; each installation site its own peculiar climatic conditions and each user his own operational requirements. Onshore (desert, city, rural, etc) and offshore (marine, platform, etc) power plant locations are characterized

by different sources of contaminant, especially in the case of windy weather due to particle dispersion caused by the wind. The three main families that cause degradation in compressor gas turbines are: (i) corrosion, (ii) erosion and (iii) fouling. Fouling mechanisms involve three specific aspects: (i) the environmental conditions (airborne contaminant, salt, etc.) in which the gas turbine operates, (ii) the power plant design and management (filtration system, washing operation, etc.) and (iii) compressor characteristics (pressure ratio, number of stages, etc.) [1]. The quality and purity of the air entering the turbine is a significant factor in its performance and life and for this reason, filtration systems that can limit the ingestion of contaminants by the power unit are required.

Fouling, and thus particle adhesion on the blade surface is a complex phenomenon that includes many aspects (materials, surface conditions, particle size and impact dynamic). Particle sticking on blade surfaces results in an increase in the thickness of the airfoil and the surface roughness. Evaluation of fouled compressors has revealed contamination both on the suction side and the pressure side of the compressor blades. This leads in particular to: (i) an increment in boundary layer thickness, (ii) a decrement in the flow passage area and (iii) modifications of 3D fluid dynamic phenomena [2, 3]. A fouling issue is classified as recoverable with cleaning/washing operations. Diakunchak [4] estimates that the extent of this type of unrecoverable deterioration is usually less than 1 %. Experimental results reported in [5] demonstrate that the process of washing was assumed to recover the output power by up to 99.5 %.

In this paper an estimation of the deposits that affect a blade surface is proposed. Climatology, filtration technology and specific studies regarding particle adhesion have to be combined in order to generate a useful approach to studying the fouling phenomenon. The quantitative analysis of the deposits on a blade surface is strongly related to realistic (i) air contamination data, (ii) filtration efficiency and (iii) particle adhesion. This analysis is conducted in a similar way to that reported by the authors in [6]. In particular, the paper is organized around the following points:

- definition of the computational strategy adopted in order to relate: (i) air contaminant concentration, (ii) filtration efficiency and (iii) particle adhesion characteristics;
- definition of the typical air contaminant concentration in the urban area as a function of (i) particle diameter and (ii) the season;
- definition of the filtration efficiency as a function of (i) particle diameter and (ii) charge level of the electrostatic filter;
- definition of the particle adhesion to the blade surface as a function of (i) particle diameter and (ii) local position on the blade surface;
- calculation of the contaminant mass on the blade surface and quantitative analysis regarding the influence of external factors (such as season and filtration system) on a fouling rate.

## **NOMENCLATURE**

$d$	diameter
$m$	mass flow rate
$n$	ratio
$P$	number of particle

## **Greek letters**

$\eta$	efficiency
$\chi$	contaminant concentration

## **Subscripts and superscripts**

ave	average value
f	filtration system
max	maximum value
min	minimum value
p	particle
peak	peak value

## **Acronyms**

CFD	Computational Fluid Dynamics
DI	Dangerous Index
IS	Industrial Spring
IW	Industrial Winter
OC	Optimal Charge
PC	Poor Charge
LE	Leading Edge
PS	Pressure Side
SEM	Scanning Electron Microscope
SP	Sticking Probability
SS	Suction Side
TE	Trailing Edge
U	Urban

## **METHODOLOGY**

The authors in [6] developed a methodology for the evaluation of the overall amount of deposit on the blade surface, which can be represented as in Fig. 1.

This methodology is based on the superposition of the deposition patterns caused by each class of particles. In fact, starting from the distribution of airborne contaminants, particles are classified into bins according to their size, and each bin is labeled by means of the characteristic diameter of the particles.

Bin populations are then reduced according to the filter efficiency referring to the bin characteristic diameter. This allows determination of the quantity of uncaptured particles entering the compressor.

Finally, the deposition signature of each particle diameter is magnified according to the amount of particle in the bin, computed according to their adhesion characteristics and summed to the others in order to obtain the overall blade deposit pattern.

Therefore, in order to perform this calculation it is necessary to gather data regarding (i) the distribution of air contaminant in the place where the gas turbine operates, (ii) the characteristics of the filtration system and (iii) the susceptibility of the blade surfaces to fouling.

**Air contaminants.** Compressor blade fouling is normally due to one or two elements. The first is solid particulate mineral and/or plant matter, and the other is carbon smoke and/or hydrocarbon fumes which create a sticky "fly paper" substance when deposited on the turbine blades. Atmospheric aerosols are constituted by a suspension of solid (smoke, fumes, fly ash, dust, etc.) or liquid (mist, fog, etc.) in the atmosphere. In general, fine particles refer mainly to a man-made action while the coarse particles refer mainly to a natural phenomenon.

Brake [7] explains the issue related to contaminant transportation in detail. A 20  $\mu\text{m}$  particle will fall at around 350 m/h. If the particle has been lifted to 2,100 m, it would take six hours to fall back to earth. A wind speed of 20 km/h would give this particle a range of 120 km. However, a 5  $\mu\text{m}$  particle in the same situation would settle at around 35 m/h, meaning it would take 60 h to fall back to earth, giving it a range of 1,200 km under the same circumstances.

The dispersed aerosols have different shapes as a function of their nature and source. In [8] there are detailed SEM pictures that report the shape of typical aerosols dispersed in the Shanghai urban summer atmosphere. The authors also report a mass characterization of the different size airborne

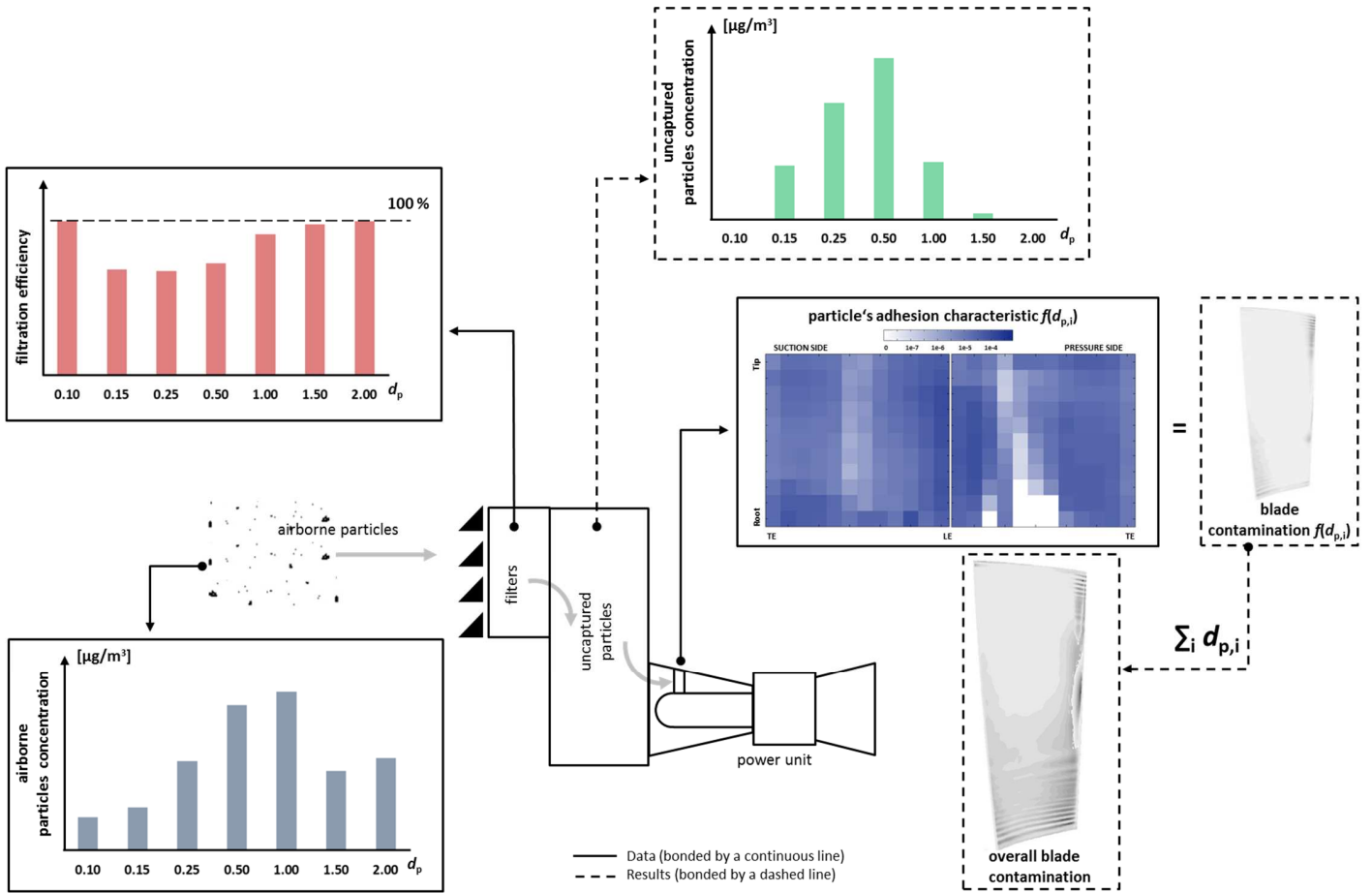


Figure 1 – Methodology for the evaluation of the overall amount of the deposit on blade surface

particles. The mass level characterization is reported in Fig. 2 and can be considered an example of the data necessary to start this analysis.

**Air filtration system.** As reported by Schroth and Cagna [10] a gas turbine with an intake volume flow of 1.5 million cubic meters per hour will swallow up to 30 trillion particles of 0.5  $\mu\text{m}$  and larger per hour. Inlet air can significantly impact the operation performance and life of the gas turbine. The

environmental conditioning of intake air for gas turbines is required for several reasons: (i) to prevent the erosion and fouling of axial compressor blades, (ii) to reduce corrosion of the compressor air path and blading, (iii) to reduce corrosion in the hot gas area, (iv) for weather protection, (v) for cooling and (vi) for sound attenuation (Hill, 1973). The positive effects of the air filtration systems are well known, but the authors also highlight the undesirable associated properties of an air cleaner, summarized as: (i) pressure losses in the induction system, (ii) the space required to install the air cleaner with its accessories, (iii) the weight the air cleaner adds to an installation, (iv) additional labor and parts required to maintain the air cleaner, (v) initial cash outlay for the air cleaner, and (vi) other structural and environmental properties [11].

The filtration system should be selected based on the operational philosophy and goals for the turbine, the contaminants present in the ambient air, and expected changes in the contaminants in the future due to temporary emission sources or seasonal changes [12]. In order to capture different types of particles, filtration systems use many different filters. Each filter has various different mechanisms working together to remove the particles. The filter media, fiber size, packing density of the media, particle size, and electrostatic charge

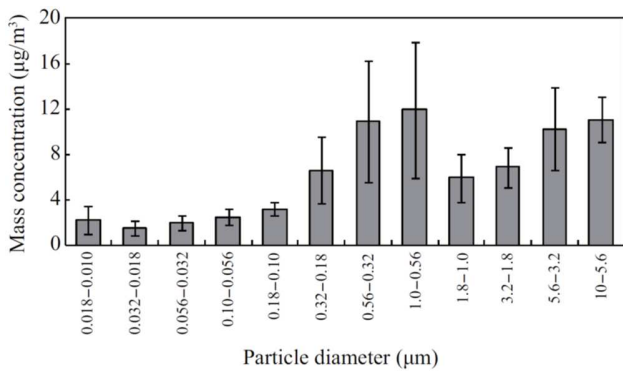


Figure 2 – Mass concentrations of size-segregated particles collected in the Shanghai atmosphere [8]

influence how the filter removes particles. The consolidated mechanisms used in air filtration systems are: (i) inertial impaction, (ii) diffusion, (iii) interception, (iv) sieving and (v) electrostatic charge. Comprehensive descriptions can be found in [12]. Particular attention is placed on the latter mechanism, related to electrostatic charge. The filter works through the attraction of particles to a charged filter. Filters always lose their electrostatic charge over time because the particles captured on their surface occupy charged sites, therefore neutralizing their electrostatic charge. When the filter is loaded, filtration efficiency increases while when the charge diminishes, filtration efficiency drops, especially for small particles. Wilcox et al. [12] pointed out that the particles with dimensions of less than  $\approx 2 \mu\text{m}$ , and, more specifically, 1, with diameters in the range of  $(0.1 - 1.0) \mu\text{m}$ , conventional filtration systems will not entirely prevent these small particles from entering the gas turbine, and therefore may cause fouling [1]. Figure 3 shows an example of filtration efficiency as a function of particle diameter and electrostatic charge (optimal and poor) based on the data reported in [12].

**Blade surface fouling susceptibility.** The first theoretical and numerical approach regarding particle deposition is provided by Agengiitürk and Sverdrup [13]. The authors presented a theory for the prediction of deposition rates of fine particles in two-dimensional compressible boundary layer flows. The mathematical model developed accounts for diffusion due to both molecular and turbulent fluctuations in the boundary layer flow. Particle inertia was taken into account for the particle flux near the surface. The theory was compared with a number of pipe and cascade experiments, and good agreement was obtained. This model was applied to a cascade turbine but represents the first theoretical and numerical model for studying particle deposition. Unfortunately, the details regarding how small particles entering the gas turbine reach the compressor blade surface and stick are not fully and quantitatively understood. All blade areas could be affected by contaminants which could stick to the blade surface, as a function of (i) the material of the body in contact, (ii) the surface conditions, (iii) the particle size, (iv) the impact velocity and (v) the impact angle.

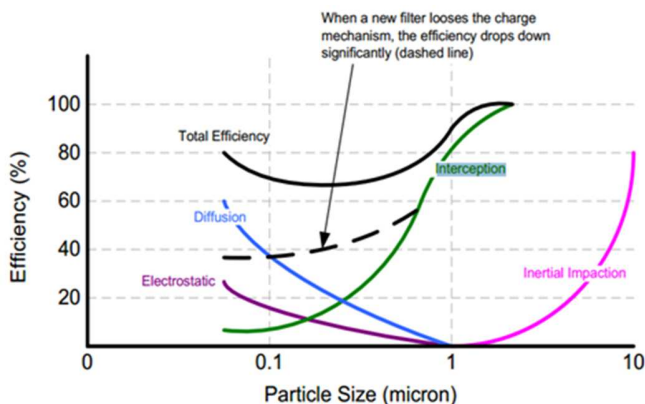


Figure 3 – Filtration efficiency values at various particle sizes as a function of the electrostatic charge [12]

On-field fouling detection [10, 11] has revealed that only the first stages are affected by deposits and, in the case of water droplets, the absence of centrifugal force in the stator vanes implies a greater number of deposits compared to the rotor vanes. The authors in [10] reported an investigation of compressor blade contamination for a Nuovo Pignone MS5322 R(B) gas turbine engine. This power unit operated for a long time without blade washing but only the first 5 to 6 stages of 16 are subjected to blade fouling due to deposits. The inlet guide vane blades, as well as the rotor and stator blades of the first stage, have more deposits on the blade suction side. The deposit masses on the blades of the other stage are approximately equal for the suction and pressure sides. The deposit masses decrease from the first to the sixth stage. From the seventh stage, the amount of deposits on blades is insignificant. The authors in [11] reported the location of salt deposits in a General Electric J85-13 axial compressor. The experimental tests have shown that the salt deposits were mainly found along the leading edge of the first four stages and on the pressure side of the stator vanes along the hub. The salt deposits were generated by the salt carried by the water droplets and, for this reason, significantly fewer deposits were observed on the rotor blades compared to the stator vanes.

Regarding the fouling application and ultra-fine powder ingestion in axial compressors, some experimental results are reported in literature [5, 12 and 13]. All of the experimental applications related to the fouling phenomenon are affected by numerous problems, summarized as follows: (i) actual conditions of the contaminants and the work environment of the compressor, (ii) size of the experimental test bench, (iii) rotational velocity of the cascade (neglected in nearly all experimental apparatus, as reported in [14]) and finally (v) the lack of particle count, in particular the lack of ratio between the injected particles and the stuck particles.

An alternative solution can be found by using the results obtained in different research fields. Inter-disciplinary research can represent a new frontier for a considerable up-grade in the investigation of fouling. In this paper the numerical results reported in [15] will be used to estimate the mass deposition on a compressor blade with the same approach reported in [6]. In [15] the authors have reported (i) an extensive analysis of the kinematic behavior of particles responsible for the fouling phenomenon and (ii) a quantitative analysis of particle adhesion. The analysis is directly related to particles which have a diameter in the range of  $(0.15 - 2.00) \mu\text{m}$  and provide the deposit mass flow rate that affects the blade surface. In order to extend the results reported in [15] (which refer to the instantaneous impact) to a realistic condition (which refers to the impact during compressor operation) the Dangerous Index (DI) proposed in [6] is adopted. The results reported in [15] are related to the experimental results reported in [16]. In particular, the results reported in [16] have particle velocity, size and materials similar to those causing fouling phenomena. The particle adhesion is established by using the sticking probability magnitude defined as a function of the normal particle impact velocity. In general, smaller particles have a

wider range of normal impact velocity and therefore there is a high probability that particle impact becomes a permanent adhesion. More details can be found in [15, 16].

### ASSUMPTIONS

In this paragraph the authors will report the data used for the estimation of the mass deposits on a blade surface.

**Air contaminant.** The data reported in Fig.2 are used in this work to analyze the mass deposits on a compressor blade surface in a configuration named Urban (U).

In order to realize as wide a fouling sensitivity analysis as possible, another mass level characterization is considered – the fact that the power units work in highly contaminated areas, due to local chimneys, plumes and/or soils. Therefore, the mass level characterization reported in [9] is also taken into account. The authors in [9] reported the air contaminant characterization of the Xuanwei, Yunnan province (China), an area characterized by pollutants emitted by local coal combustion, divided into two periods: spring season and winter season. The mass level characterization as a function of the season is reported in Fig. 4. The high concentration found in the spring time is not affected by the spore because the spore diameter is equal to 50  $\mu\text{m}$  and, therefore, out of the sampled range. These characterizations are used in this work to analyze the mass deposits on a compressor blade surface in a configuration named Industrial Spring (IS) and Industrial Winter (IW).

By using the literature data reported above [8, 9], it is possible to define the air contaminant concentration at the inlet section of the air filtration system as reported above. Table 1 summarizes the input data as a result of the classification of the particles in the bins.

**Filtration systems.** By using the literature data reported above [1, 12] it is possible to define the filtration efficiency as a function of the particle diameter. In this paper, two conditions are taken into account (see Table 2): (i) Optimal Charge (OC) condition (high efficiency) and (ii) Poor Charge (PC) condition (low efficiency) of the electrostatic filters.

As mentioned above, the particle adhesion data refers to the

**Table 1** – Mass concentration as a function of the particle diameter for U, IS and IW environment

$d_{ave}$ [ $\mu\text{m}$ ]	$\chi^U$ [ $\mu\text{g}/\text{m}^3$ ]	$\chi_{p,U}$ @ air [ $\#/\text{m}^3$ ]	$\chi^{IS}$ [ $\mu\text{g}/\text{m}^3$ ]	$\chi_{p,IS}$ @ air [ $\#/\text{m}^3$ ]	$\chi^{IW}$ [ $\mu\text{g}/\text{m}^3$ ]	$\chi_{p,IW}$ @ air [ $\#/\text{m}^3$ ]
0.15	2.50	7.2e08	16.50	8.6e09	2.00	4.4e08
0.25	1.50	3.2e08	18.50	1.2e09	2.00	1.4e08
0.50	2.00	6.6e07	35.00	1.2e08	2.00	7.8e07
1.00	2.50	9.0e06	33.00	5.4e07	2.50	1.1e07
1.50	3.25	1.3e06	39.00	7.7e06	2.00	4.8e06

**Table 2** – Filtration efficiency

$d_p$ [ $\mu\text{m}$ ]	Poor Charge	Optimal Charge
	$\eta_f$ [%]	$\eta_f$ [%]
0.15	49	68
0.25	47	67
0.50	54	72
1.00	82	91
1.50	93	98

results reported in [15], therefore the filtration efficiency is defined for the analyzed particle diameter. The filtration efficiency values as a function of the particle diameter are reported in Table 2.

Combining the mass concentration values (U, IS and IW) and the filtration efficiency (OC and PC), the contaminant concentration at the inlet section of the compressor can be calculated for the six considered cases (Table 3). In order to realize a comparative analysis, some hypotheses must be defined:

- the density of the contaminant is imposed equal to 3,000  $\text{kg}/\text{m}^3$ . This value is obtained by a mass-weighted average of the air contaminant proposed in [8, 9];
- in order to calculate the number of particles swallowed by the compressor, the volume flow rate at the best efficiency point equal to 21.26  $\text{m}^3/\text{s}$  is imposed [15].

**Particle adhesion.** The results reported in [15] refer to the particle impact (instantaneous scenario), and the sticking probability threshold limit imposed equal to 0.5 represents a useful discerning value to establish which particles stick or bounce. In order to attribute the instantaneous scenario to the time-wise scenario, the Dangerous Index (DI) is used. This index refers to a specific amount of particles (that have a non-zero value of sticking probability) that impact on a specific blade area. The Dangerous Index is defined as the product between the ratio  $n$  and the average value of the particle sticking probability  $SP_{ave}$ . The ratio  $n$  is defined as the ratio between the amount of particles that hit the blade area with a  $SP > 0$  and the amount of particles that enter the compressor. The DI values are reported in Fig. 4 by using a colored region according to the blade surface spanwise and chordwise subdivisions. Dangerous Index values vary in the range (0 – 6.5e-4). Further details related to the DI definition can be found in [6].

Results reported in [15] refer to a particle density equal to

**Table 3** – Contaminant concentration at the compressor inlet section

	$d_p$ [ $\mu\text{m}$ ]	Optimal Charge		Poor Charge	
		$\chi_p$ @ inlet [ $\#/\text{m}^3$ ]	$P$ [ $\#/\text{s}$ ]	$\chi_p$ @ inlet [ $\#/\text{m}^3$ ]	$P$ [ $\#/\text{s}$ ]
Urban	0.15	1.9e08	1.3e08	3.1e08	2.1e08
	0.25	9.0e07	6.2e07	1.5e08	1.0e08
	0.50	1.6e07	1.1e07	2.6e07	1.8e07
	1.00	7.0e05	4.8e05	1.4e06	9.4e05
	1.50	2.3e04	1.6e04	8.1e04	5.6e04
Industrial Spring	0.15	2.3e09	1.6e09	3.8e09	2.6e09
	0.25	3.5e08	2.4e08	5.6e08	3.9e08
	0.50	2.8e07	1.9e07	4.5e07	3.1e07
	1.00	4.2e06	2.9e06	8.2e06	5.6e06
	1.50	1.3e05	9.1e04	4.7e05	3.2e05
Industrial Winter	0.15	1.2e08	8.2e07	1.9e08	1.3e08
	0.25	4.0e07	2.8e07	6.5e07	4.4e07
	0.50	1.8e07	1.3e07	3.0e07	2.1e07
	1.00	8.8e05	6.1e05	1.7e06	1.2e06
	1.50	8.1e04	5.6e04	2.9e05	2.0e05

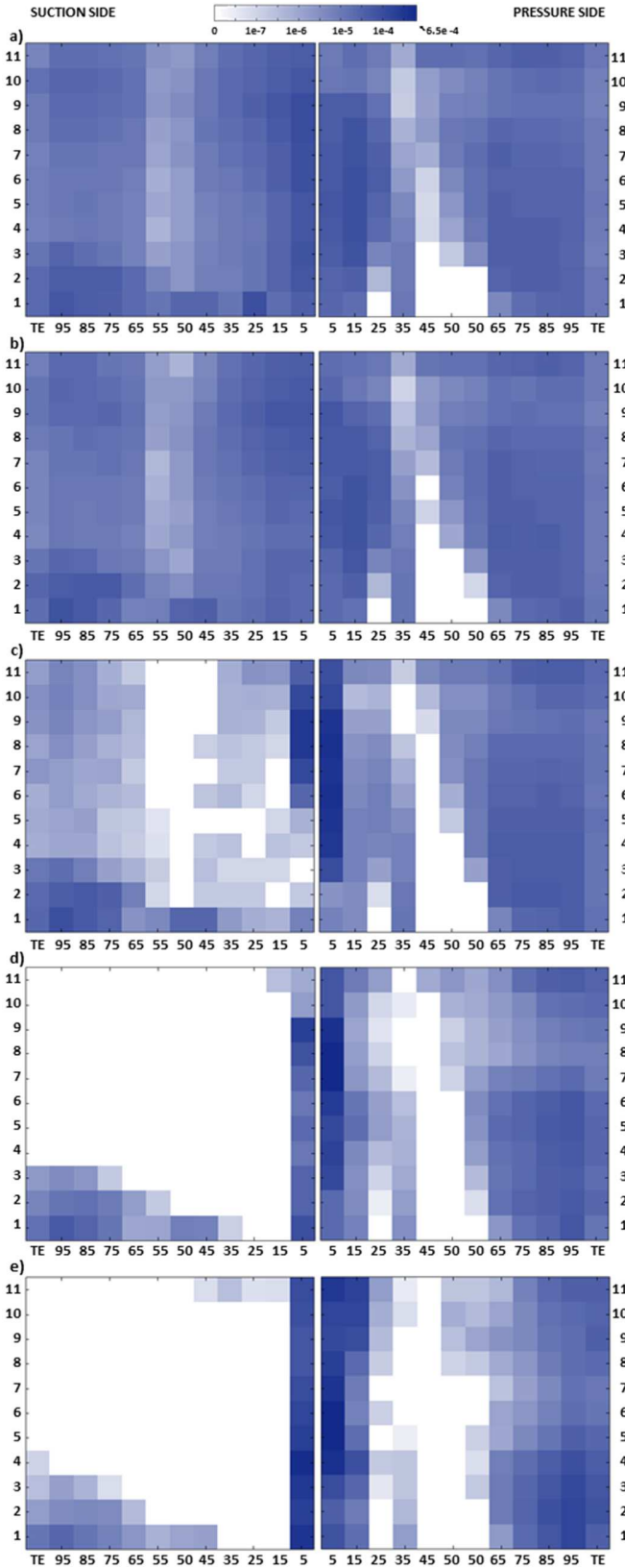


**Figure 4** – Dangerous Index maps: a)  $d_p = 0.15 \mu\text{m}$ , b)  $d_p = 0.25 \mu\text{m}$ , c)  $d_p = 0.50 \mu\text{m}$ , d)  $d_p = 1.00 \mu\text{m}$  and e)  $d_p = 1.50 \mu\text{m}$

$2,560 \text{ kg/m}^3$ , and are therefore corrected  $3,000 \text{ kg/m}^3$  and completed by the data related to the Dangerous Index for  $d_p = 1.50 \mu\text{m}$ .

In the following paragraphs the deposits on the blade surface are analyzed in two different ways: (i) deposits divided by the blade side (pressure or suction) and (ii) deposits divided by a very fine discretization of the blade surface (mesh). In Fig. 5, the mesh realized on the blade surface is reported. From Fig. 5, the subdivision of the blade surface is clearly seen as from hub to shroud with eleven strips, and from leading edge to trailing edge with twelve slices as a function of the DI maps reported in Fig. 4.

In this analysis the influence of the wetness in the passage vanes is not taken into account. In general, particles that impact on wet surface have more chance of sticking there [1] but, at the same time, the droplets which result on the blade surface (due to the humidity and/or to the inlet depression for the early stages) could drag the airborne contaminants from the rotor to the stator surfaces [10, 11]. The authors highlight that the particle characteristics used in [16] are quite different compared to the classic particle characteristics involved in fouling phenomena. In particular, the silicon carbide particles [16] have a very high level of hardness and this implies that the rebound properties could be different from those found in the real fouling applications.

## RESULTS

The results refer to two analyses. The first is the blade contamination analysis in which the sensitivity analyses as a function of the blade side (pressure or suction) are reported. The second is the calculation and representation of the overall deposits on the blade surface.

**Blade contamination.** In this section the authors have reported the analysis related to the deposits on the pressure and suction side, as a function of the conditions mentioned above.

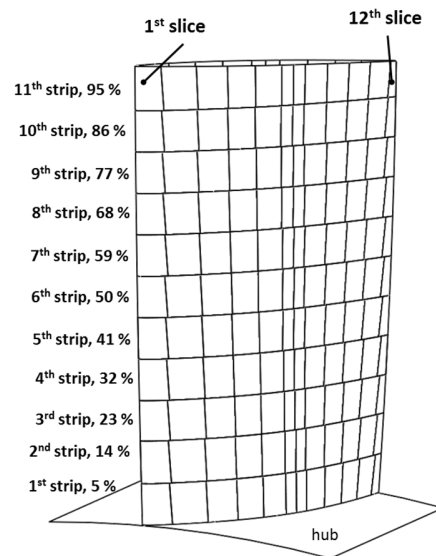


**Figure 5** – Subdivision of the blade surface: eleven strips with its correspondent average value of the blade span and twelve slices

The analysis refers to the quantification of the deposits on the blade surfaces in order to highlight which conditions are more dangerous for the compressor. As reported by Morini *et al.* [17] the same deposits generate different performance drops as a function of the blade side. The deposits on the SS are more dangerous than the deposits on the PS. The first analysis is carried out in order to set the reference. In fact, the results reported in Figs 6, 7 and 8 show the blade contamination in the absence of the filtration systems.

The values in Figs 6 – 8 are the results of the combination of contaminant concentration in the air (Table 1) and the DI values. The values refer to the mass per second which sticks to the blade surface. The considered particle diameters are those that have a filtration efficiency of less than 100 %.

From Fig. 6 it is clearly visible that in all conditions the pressure side is more contaminated than the suction side. The higher deposition on the suction side corresponds to the Industrial Spring condition, as well as on the pressure side. In this case the seasons influence both blade sides in a similar manner Industrial Spring is the most dangerous while the Urban condition is the least dangerous. The pressure side appears to be affected by deposits twice as much as the suction side.

In Figs 7 and 8 the differences in terms of particle diameter are reported for the pressure side and suction side respectively. The pressure side is more contaminated by particles with a diameter equal to 1.00  $\mu\text{m}$  in the IS condition, as well as the suction side in which the most dangerous particles have a diameter equal to 0.15  $\mu\text{m}$ . It is clearly visible how the combination of the contaminant concentration and sticking probability values (represented by the DI) determine different results as a function of the blade side. On the pressure side the bigger particles are responsible for higher blade side contamination. These particles ( $d_p$  in the range of 0.50  $\mu\text{m}$  to 1.50  $\mu\text{m}$ ) hit the pressure side with an  $SP_{ave}$  which is lower than the  $SP_{ave}$  of the smaller particles, but the higher number of impacts determine a very dangerous condition for this blade side. On the suction side the particle contributions are more similar and, fixing the condition, the dangerous diameter changes. In fact, the diameter of the dangerous particles for the IS condition is 0.15  $\mu\text{m}$ , but for the IW condition it is 1.50  $\mu\text{m}$  and finally, for the U

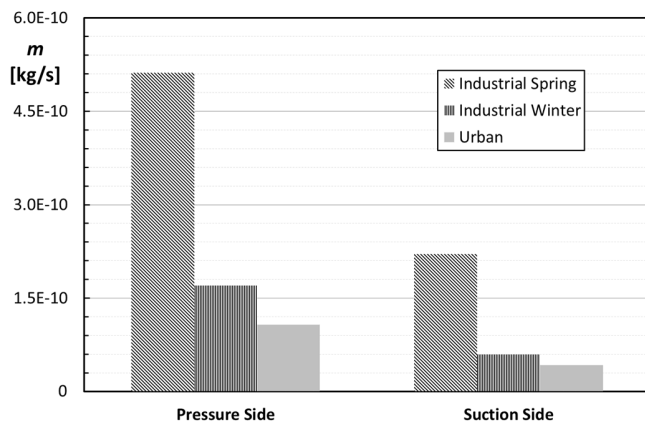


Figure 6 – Contaminant mass on the blade surface without filtration system

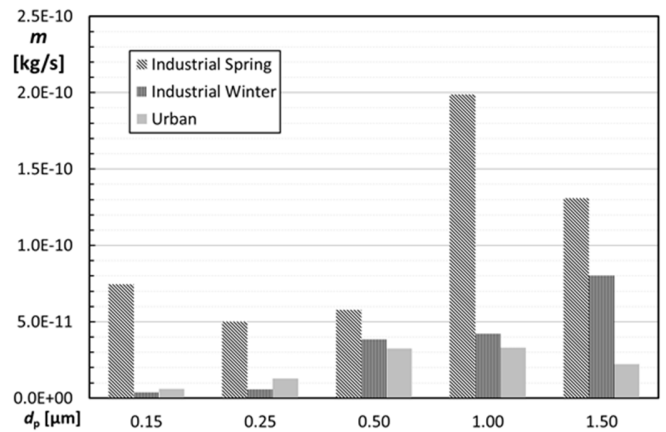


Figure 7 – Contaminant mass on the PS without filtration system

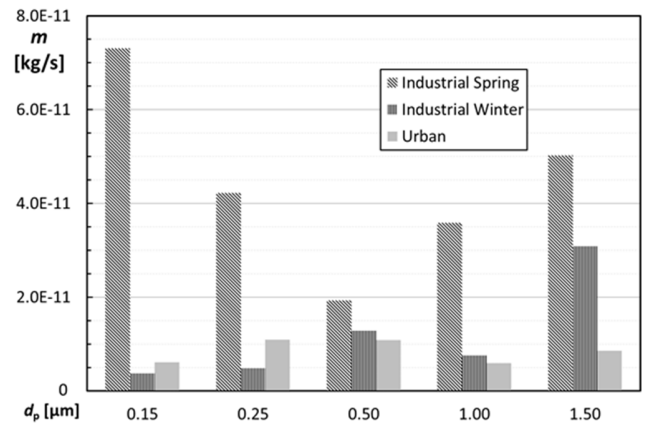


Figure 8 – Contaminant mass on the SS without filtration system

condition it is 0.50  $\mu\text{m}$ . The subsonic suction side appears more prone to collecting particles that have a wide diameter range. These results confirm the requirement of a specific design of the filtration systems related to the power plant location [12].

Figure 9 reports the results related to the blade contamination with filtration systems. Two conditions are reported: optimal charge and poor charge of the filtration system. The reduction, by using a filter with optimal charge (optimal charge conditions), is in the range of (41 – 46) % depending on the environmental conditions.

These results highlight the importance of the presence of the filtration system and its efficiency:

- the filtration system with poor charge reduces the mass contaminant by about 74 % on the pressure side and by about 68 % on the suction side with respect to the case without filtration system;
- the filtration system with optimal charge reduces the mass contaminant by about 85 % on the pressure side and by about 81 % on the suction side with respect to the case without filtration system.

Finally, it is possible to observe that the characterization of the contaminant concentration in the air is more important than

the filter charge. In fact, IW and/or U conditions in the case of poor charge, are less dangerous than the IS condition in the case of optimal charge.

In Figs 10 and 11 the differences in terms of particle diameter are reported for the pressure side and suction side respectively. The different charge condition determines a flatter

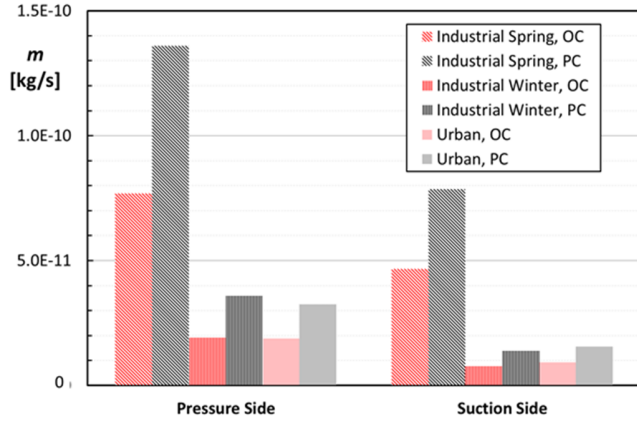


Figure 9 – Contaminant mass on the blade surface with filtration system

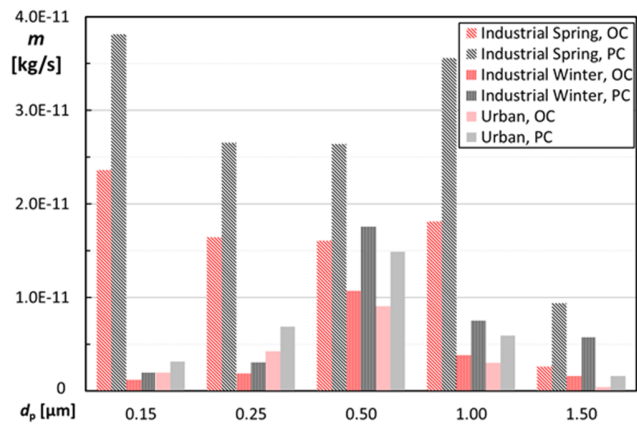


Figure 10 – Contaminant mass on the PS with filtration system

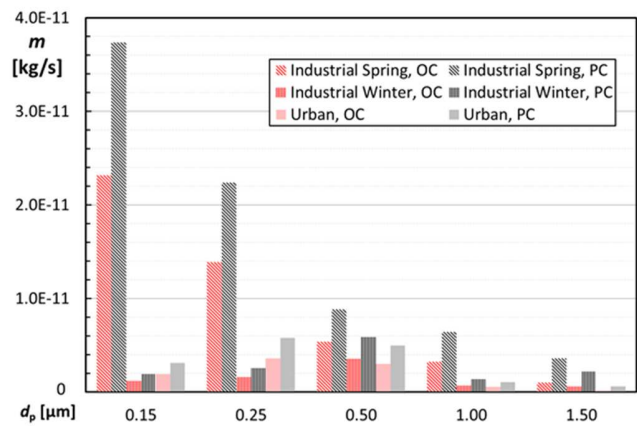


Figure 11 – Contaminant mass on the SS with filtration system

scenario with respect to the single particle diameter. This effect is more evident on the pressure side than the suction side. For example, for the IS condition, in the case of poor charge the highest contribution corresponds to  $d_p$  equal to 0.15  $\mu\text{m}$  and 1.00  $\mu\text{m}$ , while in case of optimal charge, the contributions of the particle with a diameter in the range (0.15 – 1.00)  $\mu\text{m}$  are quite similar. On the suction side the higher contribution is related to particles with a diameter equal to 0.15  $\mu\text{m}$  and 0.25  $\mu\text{m}$  during the IS condition. Regarding the suction side, it is important to emphasize that the smallest particles are the most dangerous only for the IS condition while, in the IW and U conditions, the most dangerous particles are 0.50  $\mu\text{m}$  and 0.25  $\mu\text{m}$  respectively. The suction side is contaminated in a way which is similar to the pressure side (the peak values are quite similar). This evidence is probably due to the influence of particle impact and deposition on the leading edge. In fact, as reported in [15] the thickness of the leading edge determines a high amount of particle impact that hits the blade surface in the first part of the chord equally divided between the pressure and suction side.

**Overall deposits.** In this section the authors have reported a specific analysis related to deposits on the blade surface. As mentioned above, the blade surface was divided into eleven strips along the spanwise direction, and into twelve slices along the chordwise direction. This very fine discretization of the blade surface allows the visualization of deposits which is quite similar to the real scenario.

For each considered case, the localization of the contaminant peak on the pressure side ( $m_{PS,peak}$ ) and suction side ( $m_{SS,peak}$ ) is reported. The average values of contaminant at the pressure side ( $m_{PS,ave}$ ) suction side ( $m_{SS,ave}$ ), leading edge ( $m_{LE,ave}$ ) and blade tip ( $m_{TIP,ave}$ ) are also reported. The deposits on these blade areas in fact have the greatest influence on compressor performance degradation, as reported in [17, 18].

Without filtration system. In a similar way to the analyses reported above, the first analysis is carried out in order to set the reference. In fact, the results reported in Fig. 12 show the blade contamination in the absence of filtration system. Figure 12 shows that deposits are concentrated in the first part of the airfoil chord on the pressure side. In particular the peak values are in the area of the leading edge on the pressure side and suction side at the 7<sup>th</sup> (59 % of the blade span) strip and 9<sup>th</sup> (77 % of the blade span) respectively. The deposits on the suction side are more distributed than those on the pressure side, but the average value is about 50 % of the magnitude less than the pressure side. In the case of the subsonic rotor, the average values of the blade sides are closer to each other with respect to the transonic rotor. At the blade tip, the average value of deposit is higher than the average values of the suction side. This implies that the blade tip is more fouled with respect to the suction side.

IS and poor charge. The second analysis refers to the most dangerous fouling operating condition poor charge of the filtration system and IS as the compressor work environment. Figure 13 shows the deposits on the blade surface. The color bar values are different from the previous case in order to



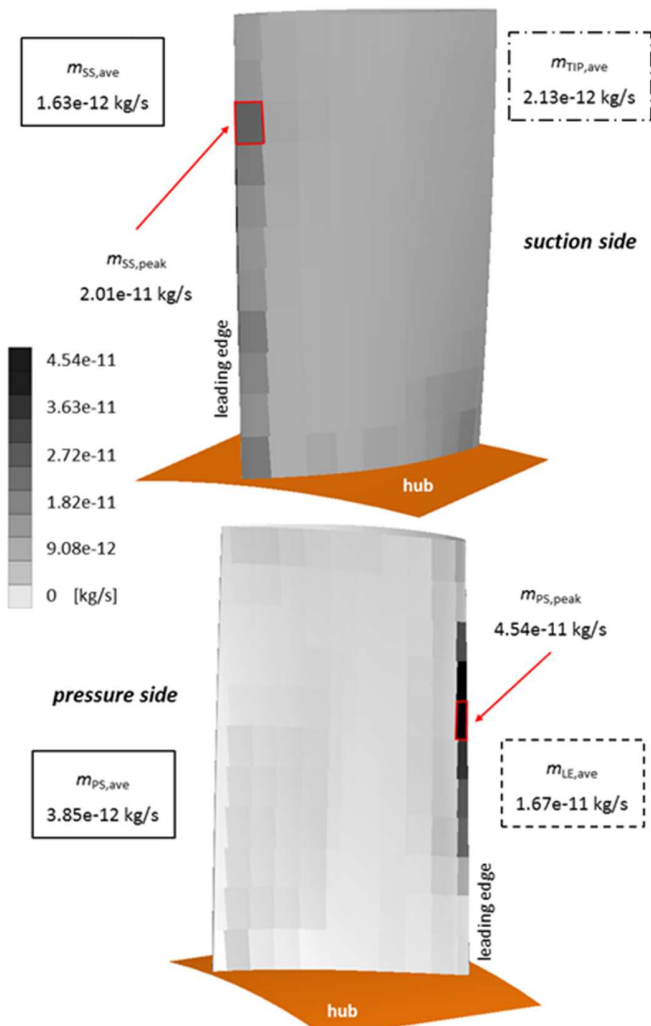


**Figure 12** – Overall deposits on the blade surface without filtration system

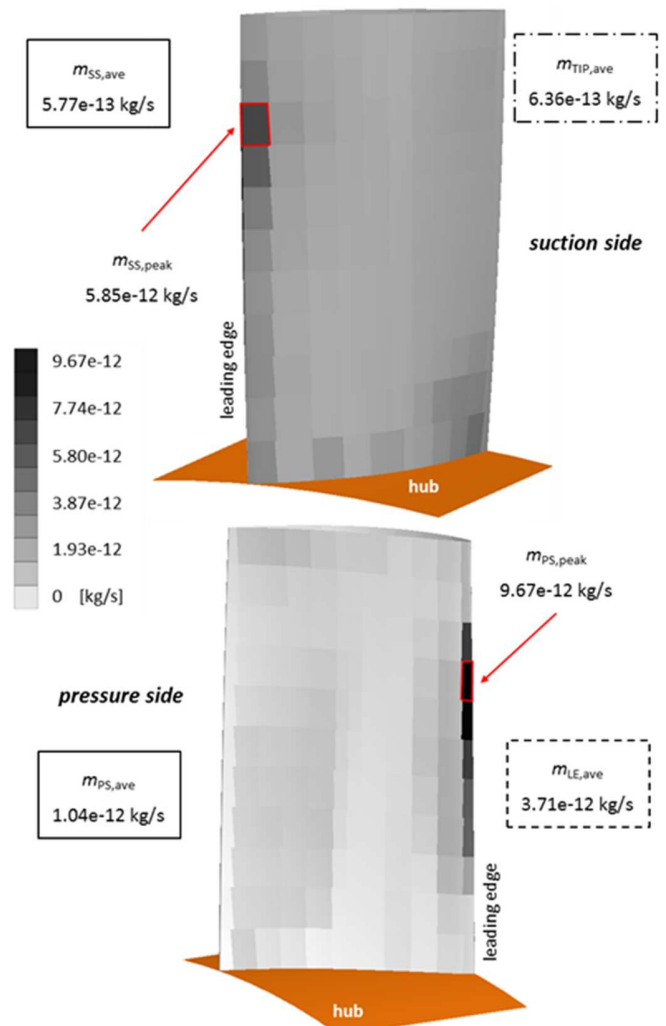


**Figure 13** – Overall deposits on the blade surface: IS and poor charge

improve contour plot readability. The color bar values used for this analysis will be held constant for all the following analyses. The peak value on the pressure side is located in the 8<sup>th</sup> strip (68 % of the blade span) with a reduction in mass contaminant of about 79 %. On the suction side, the deposit peak is located in the same region as the previous case with a reduction of about 71 % with respect to the case without a filtration system. Regarding the average values of the deposits on the pressure side and suction sides, it can be noticed that the filtration system with a poor charge realizes a reduction of about 73 % of the mass deposits on the pressure side while, on the suction side the reduction is only about 65 %.

**Industrial Spring and optimal charge.** Figure 14 shows the deposits on the blade surface in the case of IS environment with optimal charge conditions. As mentioned above, the filtration system charge reduces the amount of deposits on the blade surface. For the pressure side the average reduction is about 43 % while for the suction side the reduction is about 41 % with respect to the case with poor charge condition. The peak

values on the pressure side and suction side are in the same blade areas with respect to the previous cases (without filtration system, and IS with poor charge). On the suction side, the blade area close to the leading edge is affected by deposits in a similar way to the rear part of the airfoil chord. This phenomenon is due to the flow separation in the corner of the flow passage vane.

**IW and optimal charge.** The last analysis refers to the least heavy operating condition IW environment with optimal charge conditions. Figure 15 shows the deposits on the blade surface. As mentioned above, this condition is the least heavy of those considered. In this case, the contaminant concentration in the ingested air has a greater influence for the deposits in suction side, with the reduction in the peak value equal to 69 % for the suction side (with respect to the peak value resulting for the case IS with optimal charge), while in the pressure side the reduction in the peak value is about 67 % (with respect to the peak value resulting for the case IS with optimal charge). The same trend can be obtained by using the average values. In this

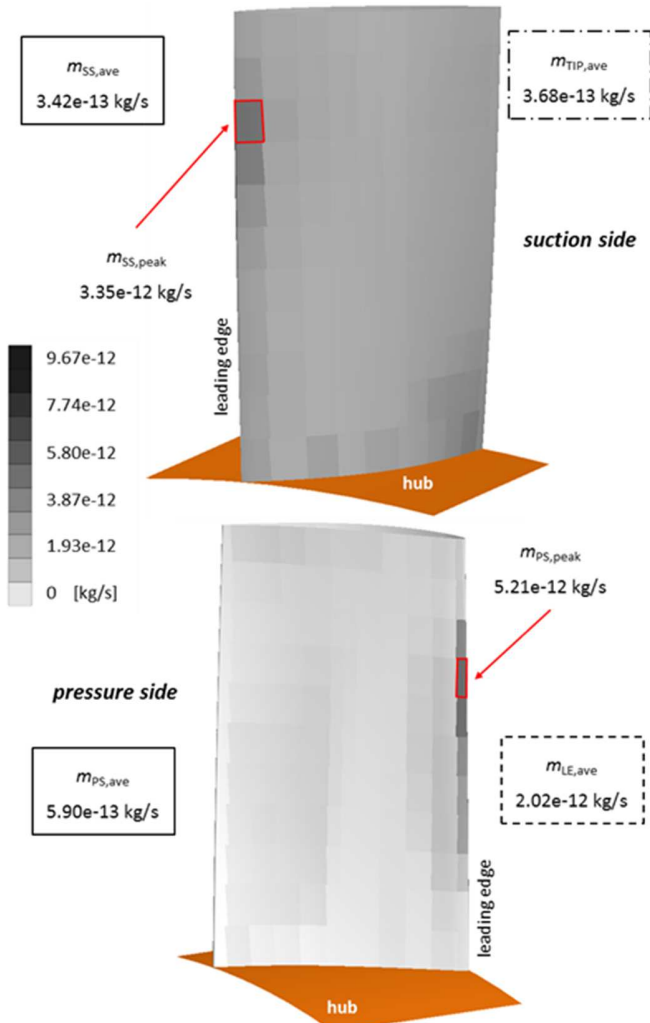


Figure 14 – Overall deposits on the blade surface: IS and optimal charge

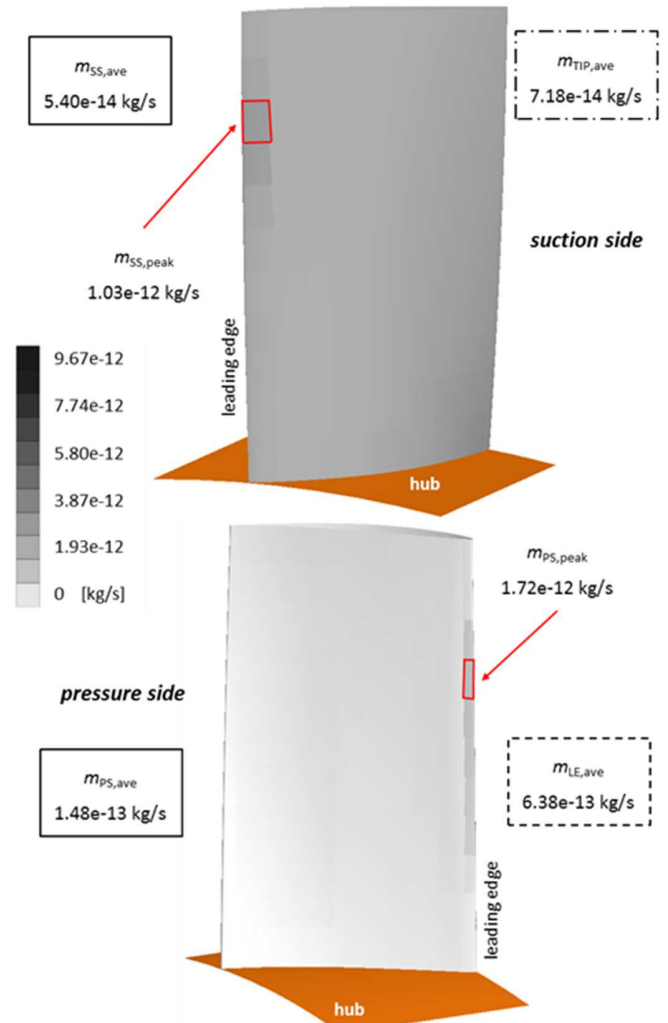


Figure 15 – Overall deposits on the blade surface: IW and optimal charge

case, the season, and also the work environment of the compressor strongly influence the deposits on the suction side.

### OBSERVATIONS AND COMPARISON

As mentioned above, the study of the particle impact/adhesion presented in this paper for a subsonic rotor is the continuation of a previous work conducted for a transonic rotor [6]. In this paragraph, the authors report a comparison between the two studies.

The values of mass deposits presented in this work are directly related to the DI. This index is strongly related to the sticking coefficient reported in [19]. By using the DI it is possible to highlight some considerations regarding the particle adhesion on the pressure and suction side.

Figure 16 shows the relationship between the DI and the particle diameter for the pressure side and suction side. The two trends are very similar especially for particles with a diameter bigger than 0.5  $\mu\text{m}$ . The two trends seem to be shifted along the ordinate axis. The separation and diffusion phenomena only

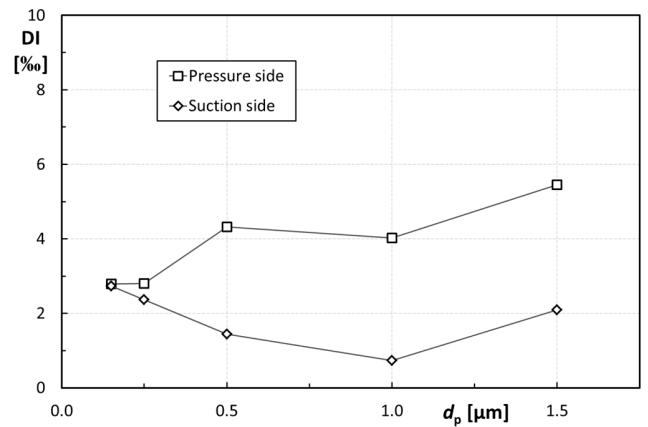


Figure 16 – DI versus particle diameter

take place in a small portion of the suction side close to the hub, and both blade sides show that the inertial deposition is the major contributor to the composition of the deposits. In

particular, as shown above, the deposition is concentrated on the leading edge area and the particle surrounds the leading edge from the suction side to the pressure side. These results are in line with those presented in [19] where the authors pointed out that only with a different deposition mechanism (inertial or diffusion), the sticking coefficient, as the DI in this paper, changes its values and trends. As highlighted in [6], in the case of the transonic rotor, where the flow field differs greatly between pressure side and suction side, the DI assumes different values and, for the suction side, DI values are smaller for bigger diameter. In this case, the suction side is in fact characterized by separation due to the shock wave and, consequently, by a turbulent and thicker boundary layer. This condition allows the diffusion-deposition condition and, as reported in literature, this condition influences the deposition of the smaller particles [12].

Given this analysis, even if (i) the particle characteristics used in [16] are different from those involved in the fouling phenomena and (ii) the simplifications adopted in this work and in [15] regarding particle density and particle diameter, the deposition trends (Fig. 16) are in agreement with the considerations reported in literature [19], demonstrating that the combination of inter-disciplinary results could be an effective strategy for investigating the fouling phenomenon.

Regarding the amount of contaminants that sticks on the blade surfaces, this is almost the same for the subsonic and transonic rotors. The order of magnitude of the contaminant is the same, especially for the pressure side. On the suction side, the subsonic rotor shows a higher peak of contaminant located in the leading edge areas near the blade tip. In this case, the smaller capture efficiency value calculated for the subsonic rotor must be related to the smaller value of the particle impact velocity, which leads to a higher value of sticking probability (and also DI). However, transonic blade surfaces appear more contaminated on the pressure side as well as on the suction side, excluding the leading edge area. The shape of the subsonic airfoils could be responsible for the higher concentration of contaminants in the leading edge areas but, at the same time, the thicker leading edge could determine fewer deposits on the rest of the blade surface.

## CONCLUSIONS

In this paper, an estimation of the actual deposits on the subsonic blade surface in terms of location and quantity is proposed. The deposits on the blade surface lead to actual (i) particle diameters, (ii) air contaminant concentrations and (iii) filtration efficiency, in order to perform a realistic quantitative analysis of the fouling phenomena.

The results show the different effects induced by the filtration system and the work environment of the compressor on the deposition rate and on the blade surface deposition pattern. The main results can be summarized as follow:

- the pressure side is more affected by the deposits in the first part of airfoil chord (close to the leading edge) at the top of the blade. Some blade areas remain almost completely free from deposits (especially in the midchord

zone, full span);

- the suction side is more affected by the deposits in the areas close to the hub for the full chord length. The leading edge represents the most fouled region;
- the filtration system influences the deposition rate. The presence and/or the operating conditions of the filtration system determine the amount of deposit that affecting each blade area.

The understanding of fouling mechanisms in compressors is still a challenge for manufacturers and users. An increase in the knowledge of fouling through the use of numerical codes may therefore constitute a decisive element for better planning of the maintenance of turbomachinery. The computational fluid dynamic numerical simulations link the design characteristics of the machine and the fluid dynamic phenomena. As shown in this work, these two items determine particle deposition on the blade surface and thus the fouling phenomena. In this sense, studies (experimental and numerical) dedicated to the interaction between the particles responsible for fouling (in terms of size and material) with blade surfaces are fundamental in order to allow for better simulations with numerical codes. This approach could be a support in the preliminary design phase, in order to establish, a priori, the cost management due to the maintenance of filtration systems, the interval for washing operations as a function of the axial compressor and the air contaminant concentration that characterizes the power plant location.

## REFERENCES

- [1] Kurz, R., Brun, K., 2012, "Fouling Mechanism in Axial Compressors", *Journal of Engineering for Gas Turbines and Power*, **134**(3), p. 032401
- [2] Suder, K. L., Chima, R. V., Strazisar, A. J., Roberts, W. B., 1995, "The Effect of Adding Roughness and Thickness to a Transonic Axial Compressor Rotor", *Journal of Turbomachinery*, **117**(4), pp. 491-505
- [3] Gbadebo, S. A., Hynes, T. P., Cumpsty, N. A., 2004, "Influence of Surface Roughness on Three-Dimensional Separation in Axial Compressors," *Journal of Turbomachinery*, **126**(4), pp. 455-463
- [4] Diakunchak, I. S., 1991, "Performance Deterioration in Industrial Gas Turbines", *Journal of Engineering for Gas Turbines and Power*, **114**(2), pp. 161-168
- [5] Viguera Zuniga, M. O., 2007, "Analysis of Gas Turbine Compressor Fouling and Washing on Line", *Ph. D. Thesis*, Cranfield University, UK
- [6] Suman, A., Morini, M., Kurz, R., Aldi, N., Brun, K., Pinelli, M., Spina, P. R., 201X, "Estimation of the Particle Deposition on a Transonic Axial Compressor Blade", *Journal of Engineering for Gas Turbine and Power*, **138**(1), p. 012604
- [7] Brake, C., 2007, "Identifying Areas Prone to Dusty Winds for Gas Turbine Inlet Specification", ASME Paper GT2007-27820
- [8] Lü, S., Zhang, R., Yao, Z., Yi, F., Ren, J., Wu, M., Feng, M., Wang, Q., 2012, "Size distribution of chemical elements and their source apportionment in ambient coarse, fine, and ultrafine particles in Shanghai urban summer atmosphere",

*Journal of Environmental Sciences*, **24**(5), pp. 882–890

[9] Lu, S., Yi, F., Hao, X., Yu, S., Ren, J., Wu, M., Jialiang, F., Yonemochi, S., Wang, Q., 2013, “Physicochemical properties and ability to generate free radicals of ambient coarse, fine, and ultrafine particles in the atmosphere of Xuanwei, China, an area of high lung cancer incidence”, *Atmospheric Environment*, **97**, pp. 519-528

[10] Schroth, T., Cagna, M., 2008, “Economical Benefits of Highly Efficient Three-Stage Intake Air Filtration for Gas Turbines”, ASME Paper GT2008-50280

[11] Mund, M. G., Murphy, T. E., 1963, “The Gas Turbine-Air-Cleaner Dilemma”, ASME Paper 63-AHGT-63

[12] Wilcox, M., Baldwin, R., Garcia-Hernandez, A., Brun, K., 2010, “Guideline for gas turbine inlet air filtration systems”, Gas Machinery Research Council Southwest Research Institute, Release 1.0

[13] Agengitürk, M., Sverdrup, E. F., 1981, “A Theory for Fine Particle Deposition in 2-D Boundary Layer Flows and Application to Gas Turbines”, *Journal of Engineering for Gas Turbine and Power*, **104**(1), pp. 69-76

[10] Tarabrin, W. P., Schurovsky, V. A., Bodrov, A. I., Stalder, J.-P., 1998, “Influence of Axial Compressor Fouling on Gas Turbine Unit Performance Based on Different Schemes and With Different Initial Parameters”, ASME Paper 98-GT-416

[11] Syverud, E., Brekke, O., Bakken, L. E., 2005, “Axial Compressor deterioration caused by Saltwater Ingestion”, ASME Paper GT2005-68701

[12] Parker, G. J., Lee, P., 1972, “Studies of the Deposition of Sub-Micron Particles on Turbine Blades”, *Proceedings of the*

*Institution of Mechanical Engineers*, **186**(1), pp. 519-526

[13] Elrod, C. E., Bettner, J. L., 1983, “Experimental Verification of an Endwall Boundary Layer Prediction Method”, Report No. AGRAD CP-351

[14] Tarabrin, A. P., Schurovsky, V. A., Boldrov, A. I., Stalder, J. -P, 1998, “An Analysis of Axial Compressor Fouling and a Blade Cleaning Method“, *Journal of Turbomachinery*, **120**, pp. 256-261

[15] Suman, A., Kurz, R., Aldi, N., Morini, M., Brun, K., Pinelli, M., Spina, P. R., 201X, “Quantitative CFD Analyses of Particle Deposition on a Subsonic Axial Compressor Blade”, *Journal of Engineering for Gas Turbine and Power*, **138**(1), p. 012603

[16] Poppe, T., Blum, J., Henning, T., 2000, “Analogous experiments on the stickiness of micron-sized preplanetary dust” *The Astrophysical Journal*, **533**, pp. 454-471

[17] Morini, M., Pinelli, M., Spina, P. R., Venturini, M., 2011, “Numerical Analysis of the Effects of Non-Uniform Surface Roughness on Compressor Stage Performance”, *Journal of Engineering for Gas Turbines and Power*, **133**(7), p. 072402

[18] Aldi, N., Morini, M., Pinelli, M., Spina, P. R., Suman, A., Venturini, M., 2014, “Performance Evaluation of Non-Uniformly Fouled Axial Compressor Stages by Means of Computational Fluid Dynamics Analyses”, *Journal of Turbomachinery*, **136**(2), p. 021016

[19] Ahluwalia, R. K., Im, K. M., Wenglarz, R. A., 1989, “Flyash Adhesion in Simulated Coal-Fired Gas Turbine Environment”, *Journal of Engineering for Gas Turbine and Power*, **111**, pp. 672-678